EFFECT OF REACTIVE AGGREGATE ON THE EARLY AGE REACTION OF WATER-GLASS ACTIVATED SLAG/FLY ASH MORTARS

Wei Wang* (1) , Shizhe Zhang (2), Ye Guang (2), Takafumi Noguchi (1)

(1). Department of Architecture, Graduate School of Engineering, The University of Tokyo, Tokyo, 113-8654, Japan.

(2). Microlab, Section Materials and Environment, Faculty of Civil Engineering and Geosciences, Delft University of Technology, Stevinweg 1, 2628 CN Delft, the Netherlands.

* Corresponding author: wangwei@bme.arch.t.u-tokyo.ac.jp

Abstract

Alkali activated materials (AAMs) have received worldwide attention due to its lower embodied energy and environmental impact than that of traditional cementitious materials. However, the activators with high alkalinity may raise the risk of alkali silica reaction (ASR) induced deterioration when reactive aggregates are used, which thereby limits the commercial use of AAMs. Not speaking the ASR induced long-term expansion, the early-age reaction of AAMs prepared with reactive aggregates is largely unknown. In this paper, isothermal calorimetry, thermogravimetry (TG) and mercury intrusion porosimetry (MIP) were adopted to study the heat evolution, mineralogical changes and pore structures of early-age ordinary Portland cement (OPC) mortar and water-glass activated slag/fly ash mortars. In each system, emphasis were made to understand the differences between mixtures prepared with standard inert quartz sands and reactive fine aggregates. The results show that the mortars prepared with reactive aggregates generated more heat in the wetting and dissolution stage. Particularly, the water-glass activated slag mortar presented the highest heat flow peak. Meanwhile, the results of TG illustrate that higher amount of reaction products were formed in water-glass activated mortars prepared with reactive aggregates than that with inert quartz sands. These findings suggest that the reactive aggregates are evidently involved in the early-age alkaline reaction of AAMs system.

Keywords: Alkaline activation; Alkali-silica reaction; Early-age; Heat evolution; Pore structure.

1. INTRODUCTION

Alkali-silica reaction (ASR), known as “concrete cancer”, is one of the main durability problems of reinforced Ordinary Portland concrete structures. ASR is a chemical reaction between alkalis in pore solution and reactive silica in aggregates [1–3]. The reaction product from ASR is a gel which will expand when it comes in contact with water. This expansion can

cause cracks in the aggregate and surrounding cement matrix [4], thereby decreasing the durability and service life of structures. Thus, it is essential to pay attention to this issue and make some precautions when reactive aggregates are used to prepare AAMs.

Up till now, a few studies have been carried out to address this potential risk of ASR in AAMs [5–13]. Although the research related to ASR in AAMs is relatively less than that of OPC system, the findings about the ASR in AAMs are always contradictory due to the different mix designs [14]. In some cases [12,14,15], the ASR-induced expansion of AAMs was very low during the standard test duration of accelerated method which was developed for traditional cementitious materials, but continued to increase if the test time was extended. This may lead to underestimating the ASR expansion of AAMs. Mahanama et al. [14] investigated the ASR-induced expansion of water-glass activated fly ash/slag blends (50 wt.% fly ash + 50 wt.% slag) by monitoring the expansion up to 150 days under accelerated condition and observed a small shrinkage in initial 21 days, followed by an exponential growth of expansion. Therefore, some researchers recommended to extend the test duration to 180 days [8].

Most of the existing researches mainly focused on the long-term ASR behaviour in AAMs, however, the role of reactive aggregates in the early-age reaction of AAMs is somehow neglected. The reactive aggregate may participate in the alkaline activation in the early-age due to the initial high alkalinity activators [8,16], and could consequently lead to differences between the long-term ASR behaviour of AAM and OPC system. The aforementioned delayed ASR expansion in AAMs may attributed to this early-age consumption of reactive aggregates. Moreover, compared to the discrepancies in the results of long-term ASR behaviour, much is unknown about the early-age reaction of AAMs mixed with reactive aggregates. Therefore, it is necessary to investigate the early-age reaction of AAMs prepared with reactive aggregates, and consequently to improve the understanding of ASR behaviour in AAMs.

In this work, the effects of reactive aggregates on the early-age reaction of OPC mortar and water-glass activated slag or fly ash were studied in terms of reaction kinetics, products and pore structures. The main aim is to investigate and to compare the role of reactive aggregates in the early-age reaction within OPC system and AAMs system. This work provides further insights for the early age ASR in AAMs and contributes to the understanding of long-term ASR behaviour in AAMs.

2. MATERIALS AND METHODS

2.1. Materials

The solid precursors used in this study were commercial ordinary Portland cement (OPC), slag (SL) and fly ash (FA), and their chemical are presented in Table 1. The mineral composition and particle size distribution of precursors are shown in Fig. 1 and Fig 2, respectively. The activator used was water-glass with a silicate modulus of 1.5 ($Ms=SiO_2/Na_2O$ by mass), which was prepared by mixing the industrial grade NaOH pellets (purity>98.5%) with industrial grade sodium silicate (Ms=3, water content=60±1%) conformed to Japanese industrial standard [17]. The activators were pre-mixed with water 24 h prior to casting to remove the effect of heat release during dilution [18].

The reactive aggregate used in this study was provided by Marushin Shitake Construction from Toyama ken in Japan. Meanwhile, the standard quartz sand per Japanese industrial standard [19] was used as inert aggregate for reference. Their chemical compositions were presented in Table 1, and mineral composition are shown in Fig. 3, respectively. The XRD patterns suggest that the reactive aggregate mainly consisted of albite; cristobalite, biotite,

clinochlore and quartz, and the amorphous content acquired by Rietveld refinement method [20] was 34.7%. The aggregates were sieved to almost same particle size distribution as shown in Fig. 4, and the D_{50} of the reactive aggregate and inert aggregate are 838.6 μm and 839.7 μm, respectively.

Table 1: Chemical composition of OPC, SL, FA and aggregates (%)

Ingredients	OPC	SL	FA	NA	RA
CaO	62.16	43.63	3.66	0.20	4.87
SiO_2	17.11	31.07	61.89	98.40	58.97
Al_2O_3	4.45	12.40	23.60	0.40	17.28
Fe_2O_3	3.00	0.32	4.50	0.40	12.02
MgO	0.83	5.45	0.94	-	2.02
Na_2O	0.39	0.25	0.04	0.01	0.71
K_2O	0.26	0.34	1.14	0.01	1.79
Na_2Oeq	0.56	0.47	0.79	0.01	1.89
MnO	0.09	0.18	0.04	-	0.18
TiO_2	0.28	0.51	1.07	-	1.01
P_2O_5	0.41	0.01	0.08	-	0.04
SO_3	2.87	1.85	0.36	-	-
Loss on ignition	2.27	0.37	2.16	0	0.89

Note: RA=Reactive aggregate; NA=inert quartz sand; $Na_2Oeq=\%Na_2O+0.658\%K_2O$.

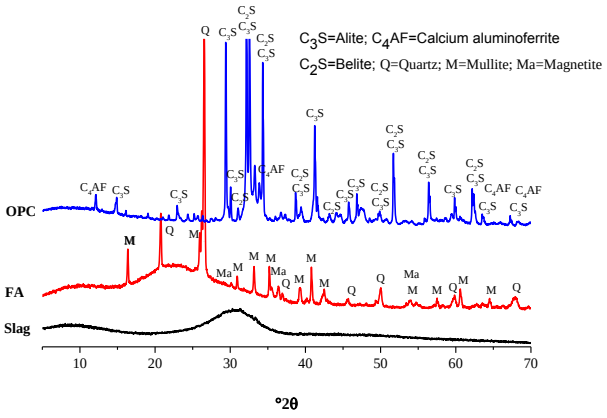

Figure 1: XRD patterns of OPC, FA and SL

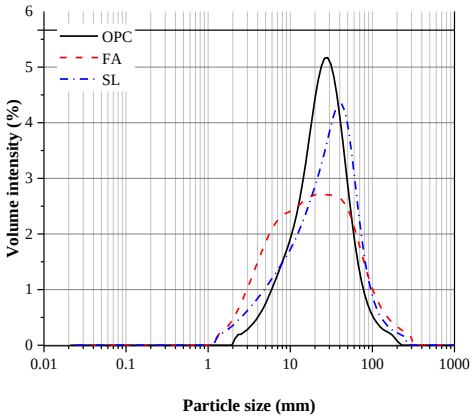

Figure 2: Particle size of solid precursors

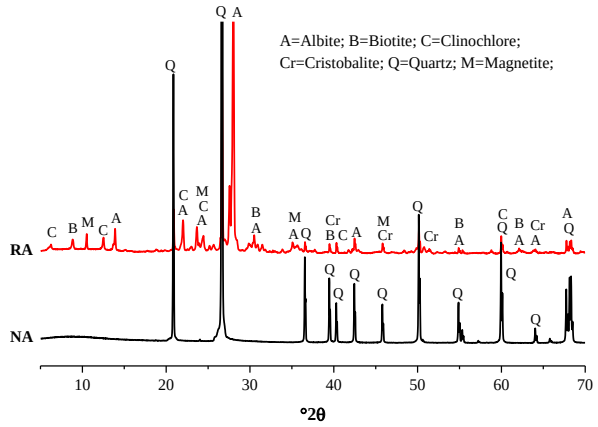

Figure 3: XRD patterns of RA and NA

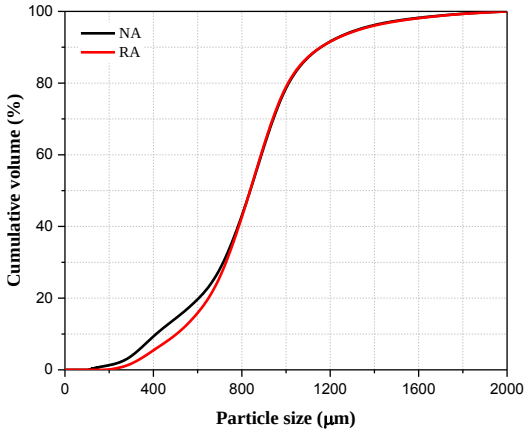

Figure 4: Pore size distribution of NA and RA

2.2. Mix design

The mix design of samples used in this study are presented in Table 2. The water to binder ratio for OPC mortars was 0.5, while the water to binder ratio of SL and FA mortars were 0.34 and activator to binder ratio were 0.5, respectively. For each group, amount of binder, water or activator were the same, only the aggregate was the variable. After casting, the specimens were cured in a climate chamber (T=20°C, RH>95%). The specimens were demoulded after 24h and were kept in the chamber until the prescribed day.

Table 2: Mixture proportions of mortars

Sample ID	Precursor	Aggregate	Aggregate/precursor	Water/cement	Activator/cement
OPC-NA	OPC	NA	1	0.5	-
OPC-RA	OPC	RA		0.5	-
SL-NA	SL	NA		0.34	0.5
SL-RA	SL	RA		0.34	0.5
FA-NA	FA	NA		0.34	0.5
FA-RA	FA	RA		0.34	0.5

Note: SL-NA represents the mixture of water-glass activated slag prepared with non-reactive aggregate; SL-RA represents the mixture of water-glass activated slag prepared with reactive aggregate. The whole of SL-NA and SL-RA were taken as AAS group, while FA-NA and FA-RA were taken as AAFA group in the following section.

2.3. Testing methods

To characterize the hydration and microstructures of mortars prepared with RA, the following instruments and methods were used. The samples used for thermogravimetry (TG) and mercury intrusion porosimetry (MIP) were cut into small pieces and immersed in alcohol for 3 days to stop hydration, followed by vacuum pumping before testing [20].

2.3.1. Heat evolution measurement

The heat evolution of different mixtures were tested using a TAM air isothermal calorimeter. The preliminary tests using internal mixing method identified the problem of clogging inside the ampoules due to the high viscosity and fast setting of AAS. Additionally, it is hard to guarantee the homogeneity of mortars by internal mixing. Therefore, the samples were mixed outside and then loaded into the TAM air isothermal calorimeter immediately after mixing. For the external mixing, it is important that the mixing time was kept the same to ensure the comparability between different specimens. The calibration was conducted at temperature of 20 °C, 48h prior to the test. The heat evolution of reaction for all mixtures were recorded for 48h.

2.3.2. Thermogravimetry (TG) analysis

TG analysis was performed using TG-DTA 2000SA system to study the amount of amorphous main hydration products in mortars at 1, 3 and 7 days. To guarantee the representativeness of samples, about 5 g samples were ground with agate mortar and approximately 50 mg powder samples were loaded in an aluminum oxide crucible. The samples were heated from 30 °C to 600 °C at a rate of 10 °C /min under 100 ml/min flow speed of nitrogen gas atmosphere.

2.3.3. Pore structures measurement

Although the MIP method has some limitations, it is still considered as an invaluable technique to study the pore structure of cementitious materials [20]. In this study, Micromeritics AutoPore III was used to investigate the pore structures of mortars prepared

with reactive aggregates or inert aggregates at 1, 3 and 7 days. The range of intruding pressure of this machine is from 3.654 kPa to 414MPa, the surface tension of mercury is 0.485N/m and the contact angle is 130 °, respectively. Thus, according to the Washburn equation [21], the pore radius can be detected ranges from 1.5 nm to 170 μm.

3. RESULTS AND DISCUSSION

3.1. Heat evolution

The effect of reactive aggregate on the early-age heat evolution of OPC, AAS and AAFA system are shown in Fig. 5. In general, the heat evolution curve can be divided into five stages [20,22], namely, initial reaction, induction period, accelerating period, decelerating period and the continued slow reaction period. As shown in Fig. 5a, for OPC system, the trend of the heat evolution curves with different aggregates are similar. This demonstrated that the effect of reactive aggregate on the early-age reaction of OPC is negligible. This may be related to the pH (approximately 12) of the pore solution in OPC system, which is mainly buffered by $Ca(OH)_2$, and the amount of $Ca(OH)_2$ in the early-age is relatively low. Therefore, the dissolution rate of silica from reactive aggregate remains low and thereby the reaction kinetic of OPC system was scarcely influenced.

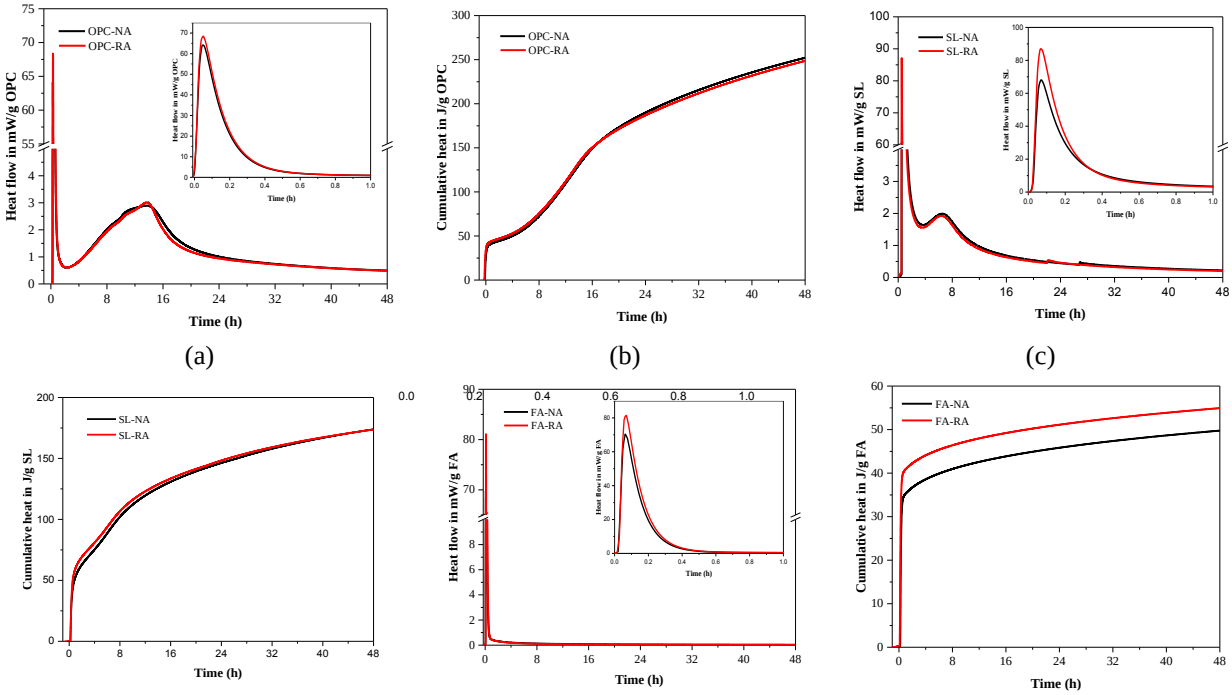

Figure 5: Heat evolution of OPC, AAS and AAFA mortars mixed with NA or RA. (AAS=waterglass activated slag; AAFA=water-glass activated fly ash)

In contrast to Fig. 5a, the first peak of heat flow curves in Fig. 5c and e were significantly affected by the reactive aggregate. For AAMs, this first peak is mainly caused by the wetting and dissolution of solid materials [23], which is similar to the initial reaction period of OPC system, but the potential physicochemical reactions are totally different. Thus, the evident increment of this peak indicated that the reactive aggregates obviously dissolved in this stage, which would influence the following chemical reaction processes and products. Meanwhile,

the heat evolution process of AAFA in Fig. 5e are different from OPC and AAS in Fig. 5a and c, it only has one peak, and no other distinct heat peak can be found. This is owing to the slow gelation and polymerization process of AAFA, which is consistent with the previous researches [24]. Additionally, very low compressive strength of early-age AAFA cured at room temperature was also reported [25,26]. As such, comparing with AAS system, the cumulative heat of AAFA after the dissolution increases only gradually and does not show tremendous increase until 48h. Nevertheless, for AAS, the heat evolution curves are similar to that of OPC system. It also has two peaks, one is before the induction period and the other is after the induction period, which is due to the high pH values (pH=14.6) of the activator used in this study [23]. However, the position and magnitude of these two peaks are different from that of OPC system as a result of different reaction mechanisms between two systems. Compared to AAFA system, it can be seen that, as time goes on, the effect of reactive aggregate on the cumulative heat of AAS gradually weaken. It is possible that the effect of reactive aggregates on the heat evolution of AAS samples might be two-edged. On the one hand, incorporating reactive aggregates prompt the dissolution heat response. On the other hand, the excessive consumption of OH^- in the dissolution stage led to the insufficient OH^- for the destruction of the bonds of other glassy phases [27] and accordingly prolonged the induction period and the corresponding heat release. This phenomenon is very similar to the effect of activator-to-slag ratio on reaction heat of AAS [23,27], which suggests that incorporating reactive aggregate acts as the role of increasing the binder content and thereby the activator-to-slag ratio of the mixture decreased. Therefore, the reaction kinetics of AAS were further influenced.

3.2. Thermogravimetric analysis

The TG and differential thermogravimetric (DTG) curves of all samples after 1, 3 and 7 days curing are presented in Fig. 6. For OPC system, there are two major peaks in the DTG curves, which is consistent with previous studies [20]. The first peak from 30 °C to 300 °C corresponds to absorbed water and the decomposition of C-S-H. The second peak between 380 °C and 500 °C is attributed to the decomposition of portlandite (CH). It is also shown that, at 1day, the weight loss of OPC-NA and OPC-RA from 30 °C to 600 °C is almost equal, and correspondingly the TG curves are almost similar. However, after 3 days curing, the difference between the curves of OPC-RA and OPC-NA were non-inevitable. This may have something to do with the amount of OH^- in pore solution of OPC system. Although the amount of CH increased with age, the solubility of CH is relatively low and thereby the pH of pore solution changes little. Therefore, the effect of reactive aggregate on hydration of OPC system is still limited.

Compared to Fig. 6a, there are only a single peak in the DTG curves of Fig 6b and c due to absence of CH in the alkali activated system [4, 36]. Previous literature suggested that this peak is mainly caused by the loss of interlayer water and dehydration of C-(N)-A-S-H type gels for AAS [29] and N-A-S-H for AAFA [30]. Therefore, that is to say, the amount of main reaction products in AAS and AAFA can be roughly reflected by the weight loss from the 105 °C to 300 °C of the TG curves in Fig. 6b and c. For AAS system, the sequence of weight loss isSL-RA-7D (4.14%) > SL-NA-7D (3.72%) > SL-RA-3D (3.37%) > SL-NA-3D (3.29%) > SL-RA-1D (2.98%) > SL-NA-1D (2.93%). For AAFA system, the sequence of weight loss is FA-RA-7D (1.51%) > FA-RA-3D (1.38%) > FA-NA-7D (1.26%) > FA-RA-1D (1.07%) >

FA-NA-3D (1.00%) > FA-NA-1D (0.75%). It clearly shows that the reactive aggregate had noticeable influence on the reaction process and promoted the gel formation.

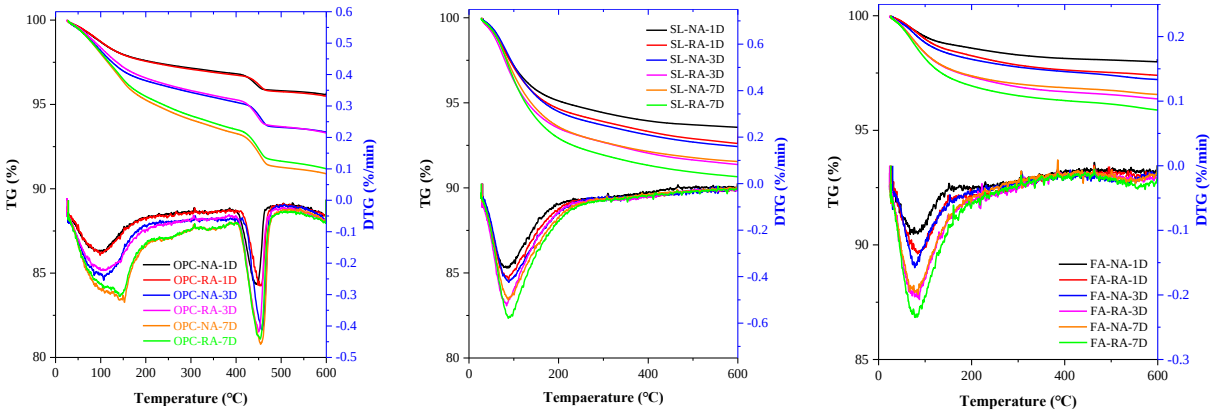

(a) OPC (b) AAS (c) AAFA

Figure 6: TG and DTG curves of OPC, AAS and AAFA mortars mixed with NA or RA.

3.3. Porosity and pore size distribution

The effect of reactive aggregate on the porosity and pore size distribution of all specimens are given in Fig. 7. With the increase of curing time, the porosity of all samples decreased gradually, except for FA-RA-3D sample. As shown in Table 3, the total porosity of FA-RA-1D and FA-RA-3D were 30.2263% and 31.0282%, respectively. The abnormal phenomenon will be explained in the following text. Meanwhile, the pore size distribution also shows refinement of pores with an increase in curing time.

For OPC system, the porosity of OPC-RA samples at 1 and 3 days were higher than that of OPC-NA, while the porosity of OPC-RA-7D was lower than that of OPC-NA-7D. In contrast to OPC, the porosity of AAS or AAFA prepared with reactive aggregate from 1 to 7 days are always greater than that of samples mixed with non-reactive aggregates. Meanwhile, the total porosity shows a strong negative correlation with the amount of reaction products. The more reaction products are, the higher total porosity is. At room temperature, the dissolution of silica from reactive aggregate is negligible [31], while it can react with the high alkaline solution in AAMs over time [32]. This may relate to the alkalinity of pore solution in corresponding samples, and this effect might be bilateral. On one hand, the high amount of OH– in the first few days accelerates the dissolution of poorly crystallized silica in reactive aggregate, and the dissolved reactive silica participated in the early-age reaction and thereby facilitated formation of reaction products. On the other hand, the dissolution of reactive aggregate leaves the hollows in the surface of aggregate, and consequently lead to the increase of total porosity [33,34]. Since the amount of OH– in OPC system is relative lower than that of AAMs [35], the reactive aggregate in AAMs were attacked more than that of OPC and thereby result in higher porosity in AAMs prepared with reactive aggregates. Particularly for AAFA, whose reaction speed is low and cannot make up the hollows in time, the results that the total porosity of FA-RA-3D was bigger than that of FA-RA-1D further reflected this effect.

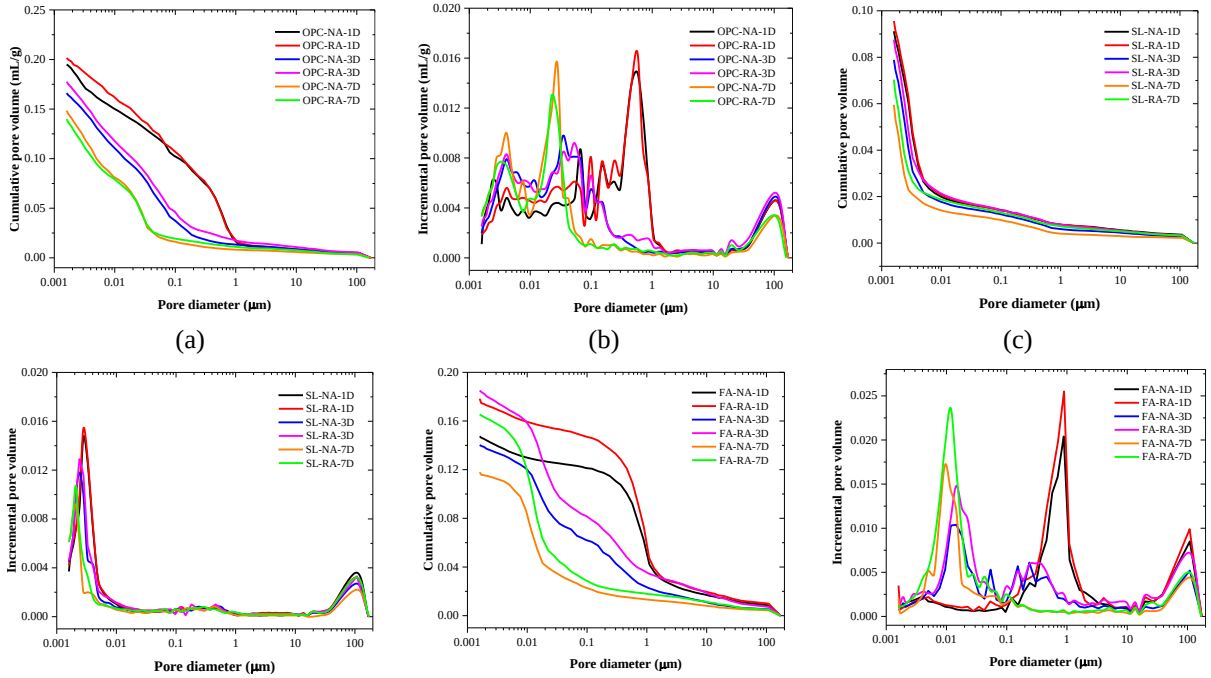

Figure7: Cumulative and incremental pore volume of OPC, AAS and AAFA mortars mixed with NA or RA

Table 3: Total porosity of samples

Sample ID	1 day	3 days	7 days
	Total porosity (%)	Total porosity (%)	Total porosity (%)
OPC-NA	34.9816	29.8330	27.6005
OPC-RA	35.4872	31.4117	25.7926
FA-NA	27.3188	26.2142	22.4827
FA-RA	30.2263	31.0282	29.1259
SL-NA	18.7866	16.4220	13.5995
SL-RA	19.3866	17.7266	14.4044

4. CONCLUSIONS

This study investigated the effect of reactive aggregates on the early-age reaction of OPC, AAS and AAFA. Based on the experiments and discussion, the following conclusions can be drawn:

(1) This study suggested that the effect of reactive aggregate on the early-age reaction of OPC, AAS and AAFA are different with each other.

(2) Compared to OPC system, the reactive aggregates in AAS and AAFA system were easier to dissolve due to the high alkaline activator and thereby generated more heat in the dissolution stage in calorimetry study.

(3) The dissolved reactive aggregate participated in the early-age reaction of AAS and AAFA, and facilitated the gel formation, which were further confirmed by TG analysis.

(4) The total porosity of AAS mortar and AAFA mortar made of reactive aggregates showed negative correlation with the amount of reaction products in early-age. The refinement of pore structure with time was also observed.

(5) The possibility of explaining the long-term ASR behavior of AAMs in terms of early-age reaction was confirmed in this study. Further cross-checking work is needed for better bridging the knowledge gap.

ACKNOWLEDGEMENT

This research is supported by Japan Society for the Promotion of Science (JSPS) and China Scholarship Council (CSC).

REFERENCES

[1] F. Rajabipour, E. Giannini, C. Dunant, J.H. Ideker, M.D.A. Thomas, Alkali-silica reaction: Current understanding of the reaction mechanisms and the knowledge gaps, Cem. Concr. Res. 76 (2015) 130–146. doi:10.1016/j.cemconres.2015.05.024.

[2] J. Lindgård, Ö. Andiç-Çakir, I. Fernandes, T.F. Rønning, M.D.A. Thomas, Alkali-silica reactions (ASR): Literature review on parameters influencing laboratory performance testing, Cem. Concr. Res. 42 (2012) 223–243. doi:10.1016/j.cemconres.2011.10.004.

[3] B. Fournier, M.-A. Bérubé, Alkali-aggregate reaction in concrete: a review of basic concepts and engineering implications, Can. J. Civ. Eng. 27 (2000) 167–191. doi:10.1139/l99-072.

[4] J.H.M. Visser, Fundamentals of alkali-silica gel formation and swelling: Condensation under influence of dissolved salts, Cem. Concr. Res. 105 (2018) 18–30. doi:10.1016/j.cemconres.2017.11.006.

[5] I. García-Lodeiro, A. Palomo, A. Fernández-Jiménez, Alkali-aggregate reaction in activated fly ash systems, Cem. Concr. Res. 37 (2007) 175–183. doi:10.1016/j.cemconres.2006.11.002.

[6] T. Williamson, M.C.G. Juenger, The role of activating solution concentration on alkali-silica reaction in alkali-activated fly ash concrete, Cem. Concr. Res. 83 (2016) 124–130. doi:10.1016/j.cemconres.2016.02.008.

[7] P. Krivenko, R. Drochytka, A. Gelevera, E. Kavalerova, Mechanism of preventing the alkali – aggregate reaction in alkali activated cement concretes, Cem. Concr. Compos. 45 (2014) 157–165. doi:10.1016/j.cemconcomp.2013.10.003.

[8] C. Shi, Z. Shi, X. Hu, R. Zhao, L. Chong, A review on alkali-aggregate reactions in alkali-activated mortars/concretes made with alkali-reactive aggregates, Mater. Struct. 48 (2015) 621–628. doi:10.1617/s11527-014-0505-2.

[9] Z. Shi, C. Shi, S. Wan, Z. Zhang, Effects of alkali dosage and silicate modulus on alkali-silica reaction in alkali-activated slag mortars, Cem. Concr. Res. 111 (2018) 104–115. doi:10.1016/j.cemconres.2018.06.005.

[10] R. Tänzer, Y. Jin, D. Stephan, Effect of the inherent alkalis of alkali activated slag on the risk of alkali silica reaction, Cem. Concr. Res. 98 (2017) 82–90. doi:10.1016/j.cemconres.2017.04.009.

[11] Y. Chen, X. Pu, C. Yang, Q. Ding, Alkali aggregate reaction in alkali slag cement mortars, J. Wuhan Univ. Technol. Sci. Ed. 17 (2002) 60–62.

[12] A. Fernández-Jiménez, F. Puertas, The alkali-silica reaction in alkali-activated granulated slag mortars with reactive aggregate, Cem. Concr. Res. 32 (2002) 1019–1024. doi:10.1016/S0008-8846(01)00745-1.

[13] R. Pouhet, M. Cyr, Alkali-silica reaction in metakaolin-based geopolymer mortar, Mater. Struct. 48 (2015) 571–583. doi:10.1617/s11527-014-0445-x.

[14] D. Mahanama, P. De Silva, T. Kim, A. Castel, M.S.H. Khan, Evaluating Effect of GGBFS in Alkali-Silica Reaction in Geopolymer Mortar with Accelerated Mortar Bar Test, J. Mater. Civ. Eng. 31 (2019) 1–11. doi:10.1061/(ASCE)MT.1943-5533.0002804.

[15] T. Bakharev, J.G. Sanjayan, Y.B. Cheng, Resistance of alkali-activated slag concrete to alkali-aggregate reaction, Cem. Concr. Res. 31 (2001) 331–334. doi:10.1016/S0008-8846(03)00125-X.
[16] A. Hajimohammadi, T. Ngo, J. Vongsvivut, Interfacial chemistry of a fly ash geopolymer and aggregates, J. Clean. Prod. 231 (2019) 980–989. doi:10.1016/j.jclepro.2019.05.249.
[17] Japanese industrial standard, Sodium silicate, 1966. doi:10.1136/jnnp.45.7.644.
[18] Z. Shi, C. Shi, J. Zhang, S. Wan, Z. Zhang, Z. Ou, Alkali-silica reaction in waterglass-activated slag mortars incorporating fly ash and metakaolin, Cem. Concr. Res. 108 (2018) 10–19. doi:10.1016/j.cemconres.2018.03.002.
[19] Japanese industrial standard, Physical testing methods for cement, Japanese Standards Association, Japan, 2015.
[20] K. Scrivener, R. Snellings, B. Lothenbach, A Practical Guide to Microstructural Analysis of Cementitious Materials, 2016. doi:10.1201/b19074.
[21] W. Gardner, The dynamics of capillary flow, Phys. Rev. 17 (1921) 273–283. doi:10.1103/PhysRev.18.206.
[22] J. Hu, Z. Ge, K. Wang, Influence of cement fineness and water-to-cement ratio on mortar early-age heat of hydration and set times, Constr. Build. Mater. 50 (2014) 657–663. doi:10.1016/j.conbuildmat.2013.10.011.
[23] C. Shi, D. Roy, P. Krivenko, Alkali-activated cements and concretes, CRC press, 2003.
[24] Z. Sun, A. Vollpracht, Isothermal calorimetry and in-situ XRD study of the NaOH activated fly ash, metakaolin and slag, Cem. Concr. Res. 103 (2018) 110–122. doi:10.1016/j.cemconres.2017.10.004.
[25]J.L. Provis, A. Palomo, C. Shi, Advances in understanding alkali-activated materials, Cem. Concr. Res. 78 (2015) 110–125.
[26] M.H. Samarakoon, P.G. Ranjith, T.D. Rathnaweera, M.S.A. Perera, Recent advances in alkaline cement binders: A review, J. Clean. Prod. 227 (2019) 70–87. doi:10.1016/j.jclepro.2019.04.103.
[27] D. Khale, R. Chaudhary, Mechanism of geopolymerization and factors influencing its development: A review, J. Mater. Sci. 42 (2007) 729–746. doi:10.1007/s10853-006-0401-4.
[28] S. Zhang, A. Keulen, K. Arbi, G. Ye, Waste glass as partial mineral precursor in alkali-activated slag/fly ash system, Cem. Concr. Res. 102 (2017) 29–40. doi:10.1016/j.cemconres.2017.08.012.
[29] X. Gao, Q.L. Yu, H.J.H. Brouwers, Reaction kinetics, gel character and strength of ambient temperature cured alkali activated slag-fly ash blends, Constr. Build. Mater. 80 (2015) 105–115. doi:10.1016/j.conbuildmat.2015.01.065.
[30] A. Fernández-Jiménez, A. Palomo, J.Y. Pastor, A. Martín, New cementitious materials based on alkali-activated fly ash: Performance at high temperatures, J. Am. Ceram. Soc. 91 (2008) 3308–3314. doi:10.1111/j.1551-2916.2008.02625.x.
[31] R.K. Iler, The chemistry of silica: solubility, polymerization, colloid and surface properties and biochemistry., Wiley Online Library, New York, 1979.
[32] J.L. Provis, J.S.J. Van Deventer, Alkali activated materials: state-of-the-art report, RILEM TC 224-AAM, Springer Science & Business Media, 2013.
[33] T. Kim, M.F. Alnahhal, Q.D. Nguyen, P. Panchmatia, A. Hajimohammadi, A. Castel, Initial sequence for alkali-silica reaction: Transport barrier and spatial distribution of reaction products, Cem. Concr. Compos. 104 (2019) 103378. doi:10.1016/j.cemconcomp.2019.103378.
[34] O. Copuroglu, Effect of silica dissolution on the mechanical characteristics of alkali-reactive aggregates, J. Adv. Concr. Technol. 8 (2010) 5–14. doi:10.3151/jact.8.5.
[35] Y. Zuo, M. Nedeljković, G. Ye, Pore solution composition of alkali-activated slag/fly ash pastes, Cem. Concr. Res. 115 (2019) 230–250. doi:10.1016/j.cemconres.2018.10.010.